Atmos. Chem. Phys. Discuss., 6, 5797–5838, 2006
www.atmos-chem-phys-discuss.net/6/5797/2006/
© Author(s) 2006. This work is licensed
under a Creative Commons License.

Atmospheric Chemistry and Physics Discussions

The influence of African air pollution on regional and global tropospheric chemistry

A. M. Aghedo[1,2], **M. G. Schultz**[1,*], **and S. Rast**[1]

[1]Max Planck Institute for Meteorology, Hamburg, Germany
[2]International Max Planck Research School on Earth System Modelling, Hamburg, Germany
[*]now at: ICG-II, Research Centre, Jülich, Germany

Received: 3 May 2006 – Accepted: 15 May 2006 – Published: 4 July 2006

Correspondence to: A. M. Aghedo (adetutu.aghedo@zmaw.de)

Abstract

We investigate the relative importance of African biomass burning, biogenic volatile organic compounds (VOC), lightning and anthropogenic emissions to the tropospheric ozone budget over Africa and globally using a coupled global chemistry climate model. Our model studies indicate that the photochemical surface ozone concentration may rise by up to 50 ppbv in the burning region during the biomass burning seasons. Biogenic VOCs contribute between 5–20 ppbv to the near surface ozone concentration over the tropical African region. The impact of lightning on surface ozone is negligible, while anthropogenic emissions contribute a maximum of 10 ppbv to the surface ozone over Nigeria, South-Africa and Egypt. The annual average of the surface and column ozone over Africa shows that biomass burning is the single most important emission source affecting the African region, while biogenic emissions have the highest contribution during the rainy seasons. The contributions of African emissions to global tropospheric ozone burden (TOB) are about 9 Tg, 13 Tg, 8 Tg and 4 Tg for African biomass burning, biogenic VOC, lightning and anthropogenic emissions respectively. These correspond to 2.4%, 3.4%, 2.1% and 1% of the global tropospheric ozone budget respectively. Over Africa itself, the contribution of each of these emission types is only 2.4 Tg, 2.2 Tg, 1.4 Tg and 0.8 Tg respectively. Outside the continent, African biogenic VOC emissions yield the highest contribution to the TOB. Our model calculations suggest that about 70% of the tropospheric ozone produced from emissions in Africa is found outside the continent, thus exerting a noticeable influence on a large part of the tropical troposphere. Latin America experiences the highest impact of African emissions, followed by southeast and south-central Asia, Oceania, and the Middle East for all the emission categories; while Canada, the United States, Russia, Mongolia, China and Europe experience the least impact of African emissions.

ACPD

6, 5797–5838, 2006

1 Introduction

Tropospheric ozone is a greenhouse gas that affects the radiative forcing and has a potential impact on the climate (Wang et al., 1980; Hansen et al., 2002). Close to the boundary layer, high ozone concentrations in the air have been shown to cause asthma attacks and pulmonary damage (e.g. Peden, 2001; Desqueyroux et al., 2002; Mortimer et al., 2002). In addition, they also damage agricultural crops and other vegetation (e.g. Mauzerall and Wang, 2001; Oksanen and Holopainen, 2001). Therefore in this paper, we analyze the impact of African emissions on the photochemically produced ozone, both over the African continent and in the global troposphere.

Air pollution emitted in Africa comes from four sources, mainly biomass burning, natural emission from vegetation and soil, lightning NO_x emission, and other anthropogenic sources – such as emissions related to the combustion of fossil-fuel for energy, industrial, transport and domestic uses. Africa contributes a significant amount to the global emissions from the first three categories, while emissions from fossil fuel combustion are important only on the regional scale.

African biomass burning activities, generally categorised as savanna, forest and agricultural waste burning, are driven by the "slash and burn" agricultural practices that take place during the dry seasons – late November to early March in the northern hemisphere (NH), and July to October in the southern hemispheric (SH) part of Africa (Marenco et al., 1990). The seasonal variation of these three biomass burning categories are responsible for the observed seasonal variation in the biomass burning emissions. In some studies (e.g., Marufu et al., 2000), emissions from the combustion of biofuel for domestic purposes are included in the biomass burning category, but in this study, they are classified as anthropogenic emissions. The estimates of the global biomass burning CO emissions range between 103–686 Tg (C) yr^{-1} (Crutzen et al., 1979; Crutzen and Andreae, 1990; Andreae, 1993; Marufu et al., 2000; Schultz et al., 2006[1]), accounting for at least 50% of the global CO emissions. Marufu et al. (2000)

[1]Schultz, M. G., Heil, A., Hoelzemann, J. H., Spessa, A., Thonicke, K., Goldammer, J.,

show that global biomass burning CO, NMHC and NO_x emissions of 287 Tg (C) yr^{-1}, 52 Tg (C) yr^{-1} and 8 Tg (N) yr^{-1} respectively, contribute about 16% to the 26 Tg TOB over Africa, and that this fraction can be up to 24% in the planetary boundary layer.

Lightning produces NO_x, mostly in the middle to upper troposphere (Ridley et al., 1996; Pickering et al., 1996, 1998; DeCaria et al., 2000), where it has a longer lifetime and greater ozone production potential than at the lower troposphere (Liu et al., 1987; Pickering et al., 1990). Lamarque et al. (1996) show in a model study that lightning is the largest contributor to the upper tropospheric tropical NO_x concentration. The total contribution of lightning to the global NO_x budget is highly uncertain. Estimates range from 2–20 Tg (N) per year (Lawrence et al., 1995; Price et al., 1997; Huntrieser et al., 2002). However, several studies published after 2000 have suggested an estimate closer to the lower limit. Huntrieser et al. (2002) estimated about 3 Tg (N) yr^{-1} from lightning NO_x based on detailed analysis of airborne NO_x measurements of European thunderstorms. Tie et al. (2001) and Martin et al. (2002) found that using a global lightning emission value of 7 Tg (N) yr^{-1} and 6 Tg (N) yr^{-1} respectively, their model simulations show reasonable agreement with airborne observations of reactive nitrogen species. Lightning activity is maximum in the tropics. However, tropical thunderstorms are the least well characterized, therefore, the uncertainty of tropical lightning NO_x is particularly large. Recent studies have shown that lightning NO_x can cause a significant enhancement of ozone in the middle to the upper troposphere. For example, DeCaria et al. (2005) calculated a photochemical ozone enhancement of about 2 ppbv during the lifetime and 10 ppbv after 24 h of a storm observed during the Stratosphere-Troposphere Experiment: Radiation, Aerosols and Ozone (STERAO-A) using a 3-D cloud-scale chemical transport model (CTM). Brasseur et al. (1996) simulated an increase of 12% in the global tropospheric ozone if lightning NO_x is doubled from 5 Tg (N)/yr to 10 Tg (N)/yr.

Vegetation emits a wide range of volatile organic compounds (Kesselmeier and

Held, A. C., and Pereira, J. M.: Global Emissions from Wildland Fires in 1960 to 2000, Global Biogeochem. Cycles, in review, 2006.

Staudt, 1999). Among these biogenic VOCs, isoprene is one of the most important (e.g., Fehsenfeld et al., 1992; Guenther et al., 1995). Biogenic VOCs can have a significant impact on tropospheric chemistry as soon as they are released into the air, because of their high reactivity. They lead to the production (or destruction) of ozone in high (or low) NO_x condition. Estimating the amount of biogenic VOC emissions is a challenging task, and up until the present, uncertainties exist (e.g. Guenther et al., 2006). The former estimate of global isoprene emission varies between 200 Tg and 570 Tg (Kesselmeier and Staudt, 1999, and references therein). The Model of Emissions of Gases and Aerosol from Nature (MEGAN) (Guenther et al., 2006) yields an estimate of about 600 Tg of isoprene, of which Africa contributes about 120 Tg (Aghedo et al., 2005). Wang and Shallcross (2000) found an increase in surface ozone concentration of about 4 ppbv over the ocean and about 8–12 ppbv over the mid-latitude land areas when isoprene emissions were included in their 3-D model simulations. Using a biogenic methanol (CH3OH) emission of 117 Tg (C) yr^{-1}, Tie et al. (2003) calculated an increase of about 3–4% in the tropical ozone at 300 hPa.

A brief description of our model and the setup of the simulation experiments are given in Sects. 2 and 3 respectively. We discuss the results in Sect. 4 and the conclusions are presented in Sect. 5.

2 The global chemistry climate model MOZECH

The full description of MOZECH and its sensitivity to the use of different emission inventories can be found in Rast et al. (2006)[2], this paper is henceforth referred to as Rast et al. (2006)[2]. The 3-D global chemistry climate model MOZECH is part of the Max Planck Institute, Hamburg Earth System Model (ESM) and consists of the 3-D global general circulation model (GCM) ECHAM5 (Roeckner et al., 2003) and the 3-D

[2]Rast, S., Schultz, M. G., Aghedo, A. M., Diehl, T., Rhodin, A., Schmidt, H., Stier, P., Ganzeveld, L. and Walters, S.: Sensitivity of a chemistry climate model to changes in emissions and the driving meteorology, in preparation, 2006.

global CTM, MOZART2 (Horowitz et al., 2003), with some modifications to the parameterizations of dry and wet deposition, surface ultraviolet (UV) albedo, and lightning NO_x production.

2.1 Chemistry scheme

The MOZECH model uses the MOZART2 tropospheric chemistry scheme, consisting of 63 transported species and 168 chemical reactions. The details of the chemical species, reactions, kinetic equations and the chemistry solver are described in Horowitz et al. (2003). As in the original MOZART model, the MOZECH chemical reaction scheme is flexible due to the MOZART2 preprocessor production of machine dependent optimized (e.g. vectorized and parallelized) code for a specific set of user-defined reactions. An implicit Euler method is applied for the integration of the kinetic nonlinear differential equations for most of the species. The MOZECH model employs a consistent link of the chemistry calculation with the parameterization of the dynamics and the physics of the ECHAM5 model.

2.2 Atmospheric dynamics

ECHAM5 (and thus MOZECH) can be run as a coupled ocean-atmosphere model or in an atmosphere-only mode. In this study, we have constrained the sea surface temperature (SST) and sea ice (SIC) by fields derived from coupled model simulations performed in the framework of the fourth IPCC assessment report (Roeckner et al., 2006). Prognostic equations for vorticity, divergence, logarithm of surface pressure and temperature expressed in spectral coefficients are solved in the dynamical core of ECHAM5. The vertical axis uses a hybrid terrain-following sigma-pressure coordinate system (Simmons and Burridge, 1981). The model uses a semi-implicit leapfrog time integration scheme (Robert et al., 1972; Robert, 1981, 1982) using a special time filter (Asselin, 1972). Details of the physical parameterizations including radiation, surface processes such as heat and water budget, gravity wave drag, cumulus convection,

stratiform cloud formation, orbit variations, and subgrid scale orography can be found in Roeckner et al. (2003).

2.3 Tracer transport and deposition

Tracers in MOZECH undergo advective and convective transport, vertical diffusion, dry and wet deposition, and chemical reactions in the atmosphere. The advection of tracers is based on a mass conserving flux-form semi Lagrangian transport scheme (Lin and Rood, 1996) on a Gaussian grid (Arakawa C-grid, Mesinger and Arakawa (1976)). Convective transport is parameterized according to the mass-flux algorithm of Tiedtke (1989) with modifications proposed by Nordeng (1994). MOZECH extends the vertical diffusion equations of ECHAM5 to include the net flux of tracers at the earth's surface (e.g emission and dry deposition). The dry deposition is according to the scheme of Ganzeveld (2001). The wet deposition is based on the wet deposition scheme of Stier et al. (2005), with modifications for below-cloud scavenging for species like HNO_3 using the model described in Seinfeld and Pandis (1998), page 1003. This dynamical wet deposition scheme takes into consideration the solubility of the tracers and the possibility of the release of trace gases into the atmosphere by re-evaporation of precipitation.

2.4 Lightning emissions

MOZECH includes an interactive lightning NO_x emissions according to the parameterization of Grewe et al. (2001). The lightning frequency is calculated as a function of the mean updraught velocity in a convective column. The NO_x emissions are proportional to the calculated flash frequency and are distributed vertically in the atmosphere using C-shaped profiles for tropical and extratropical continental and marine clouds as described in Pickering et al. (1998). Lightning emissions are subject to natural interannual variability. The calculated global lightning NO_x is about 2.7 Tg (N)/yr. This is close to the value of 3 Tg (N)/yr estimated by Huntrieser et al. (2002). Over Africa, total

lightning emissions are about 0.7 Tg (N)/yr.

2.5 Biogenic emissions

In this study, we use the prescribed biogenic VOC emissions that were used in the recent international IPCC/ACCENT intercomparison experiment (Stevenson et al., 2006). The biogenic VOC emissions are 756 Tg (C) yr^{-1}, 68 Tg (C) yr^{-1}, and 8 Tg (N) yr^{-1} for non-methane hydrocarbons (NMHC), CO and NO_x respectively. Isoprene, terpenes, methanol and other VOCs contribute about 68%, 17%, 11% and 4% respectively to the NMHCs. As an alternative to prescribed globally-gridded biogenic VOC emissions, MOZECH offers the option of an online calculation of biogenic VOC emissions according to the Model of Emissions of Gases and Aerosols from Nature (MEGAN) (Guenther et al., 2006).

2.6 Other emissions

The MOZECH model needs gridded emission data for emissions that are not calculated interactively. Emissions such as biomass burning (all open fires including savanna, forest, and agricultural burning), aircraft, soil emissions, and all other anthropogenic emissions (such as fossil-fuel combustion by the domestic, transport and industrial sector) are prescribed to the MOZECH model as monthly-mean globally gridded files. They are injected into the model at various model heights (Rast et al., 2006[2]).

With the exception of the lightning emissions, which are calculated from the interactive lightning parameterization in MOZECH as discussed in Sect. 2.4, all emissions used for this study are identical to those used for recent simulations performed in the framework of the international IPCC/ACCENT intercomparison experiment, where 25 global chemistry transport and general circulation models (including MOZECH) submitted results for a number of prescribed emission and climate scenarios (Stevenson et al., 2006). These data sets are a combination of emission inventories of the Institute for Applied System Analysis (IIASA), the Global Emissions Inventory Activity (GEIA), the

ACPD
6, 5797–5838, 2006

Global Fire Emissions Database (GFED) version 1 (Randerson et al., 2005) and the Emissions Database for Global Atmospheric Research (EDGAR) version 3.2 (Olivier et al., 1999).

Anthropogenic CO, NO_x and NMHC emissions such as domestic, industrial, road transport, off-road and power-plants fossil-fuel combustion and gas flaring are as calculated by the IIASA global version of the Regional Air Pollution Information and Simulation (RAINS) model (Amann et al., 1999) for the year 2000. The international shipping CO, NO_x and NMHC emissions are based on the EDGAR3.2 global emission inventory (Olivier et al., 1999), while aircraft NO_x emissions are specified according to the IPCC special report on Aviation and the Global Atmosphere (IPCC, 1999).

The biomass burning emissions, which include savanna, forest fires, deforestation fires, and agricultural waste burning are from the GFED version 1 (Randerson et al., 2005) database available at http://daac.ornl.gov/. For the simulations, we use the 1997–2002 monthly average data. Ocean CO and soil CO, H_2 and NO_x emissions are from the GEIA database (see Horowitz et al., 2003). The biogenic VOC emission from vegetation is based on the global model of natural VOC contributed to the GEIA activity by Guenther et al. (1995).

Table 1 lists the global CO, NO_x and NMHC emissions by source used in this study. The amounts contributed by African emissions are listed in Table 2.

MOZECH can be run in various horizontal resolutions such as T42 (~2.8°×2.8°), T63 (~1.9°×1.9°) and T106 (~1°×1°) using 19 or 31 σ-hybrid vertical levels and standard ECHAM5 time steps. The time step depends on both horizontal and vertical resolutions; for L19, it is 30, 20 and 10 minutes while for L31, it is 20, 12 and 6 minutes for T42, T63 and T106 respectively. The effect of varying model resolutions on simulated climate and on transport of tracers are described respectively in Roeckner et al. (2006) and Aghedo et al. (2006)[3].

[3]Aghedo, A. M., Schultz, M. G., and Sebastian, R.: Sensitivity of tracer transport to model resolution and forcing data in the general circulation model ECHAM5, in preparation, 2006.

3 Model simulations

The model experiments follow the general setup for the international IPCC/ACCENT intercomparison experiment (Stevenson et al., 2006). The experiments were run for present-day climate and emissions. The climate conditions (sea surface temperatures and sea ice fields) were taken from coupled ocean-atmosphere simulations performed at the Max Planck Institute for Meteorology, Hamburg. Present-day constant concentrations of 1760 ppbv, 367 ppm and 316 ppbv were maintained for CH_4, CO_2 and N_2O respectively.

Each experiment was run in the T42L31 resolution (approximately 2.8°×2.8°) for 5 years (1997–2001) after a spin-up of 6 months. We performed a reference experiment and 4 sensitivity experiments. The reference experiment includes all the emissions (this experiment is fully described in Rast et al. (2006[2]), while in each of the sensitivity experiments, we exclude only African biomass burning, biogenic VOC, lightning, or anthropogenic emissions, respectively. The differences between the reference and the sensitivity experiments therefore show the impact of each of the African emissions.

We are aware that setting an emission source to zero affects the lifetime of other trace species in the troposphere. Nevertheless, this approach provides a relatively uncomplicated method in assessing the potential impact of these different emission types. Also, the method has the advantage that the combined effect of different species (e.g CO, NO_x and NMHC) from the same emission category (e.g biomass burning) on the overall tropospheric chemistry can be assessed. The methane lifetime (average of 6.5 years based on a 200 hPa tropopause) shows small increase of about 12, 31 and 46 days in the experiment without anthropogenic, biomass burning and lightning respectively, when compared to the reference experiment. The difference between the reference experiment and the experiment where biogenic VOC emissions are switched off yields a decrease of only 37 days in the methane lifetime.

ACPD
6, 5797–5838, 2006

EGU

4 Results and discussions

In Sect. 4.1, we compare the ozone concentration calculated by the MOZECH model to in-situ aircraft ozone measurements. In Sects. 4.2 and 4.3, we discuss the impact of African emissions on the photochemical ozone production over Africa and globally. For the analysis, we consider the impact on the surface ozone concentration and the tropospheric ozone burden (TOB). The impact on the surface ozone is important because this provides the quantification of the direct impact on humans and vegetation. The TOB are necessary in determining the influence of each of the African emission categories on the entire troposphere.

4.1 Model validation

A study showing the response of MOZECH to different emissions can be found in Rast et al. (2006[2]). Here, we validate the model simulated ozone concentration of the reference simulation, by comparing it with in-situ aircraft data of the Measurement of OZone and water vapour by Airbus In-service airCraft (MOZAIC) (Marenco et al., 1998; Thouret et al., 1998a, 2006; Zbinden et al., 2006). MOZAIC has been shown to have good agreement with ozone sounding network data (Thouret et al., 1998b), this increases our confidence in using this data for the validation of our model results.

Figures 1 and 2 show the comparison of the MOZECH reference simulation and MOZAIC ozone vertical profiles for Cairo (Egypt), Abidjan (Cote d'Ivoire), Lagos (Nigeria), Johannesburg (South Africa), Caracas (Venezuela), Washington D.C. (United States), Frankfurt (Germany), Paris (France), and Osaka (Japan) for the months of January and July, respectively. The stations are chosen in such that there is at least one representative in each continental region, in this way we ensure that the entire world is covered.

For most stations, the model shows a reasonable level of agreement with the measurements in the free troposphere (800–300 hPa). The few exceptions, however, are over Caracas in January and Cairo and Johannesburg in July, where the model con-

centration is more than 25% higher than the measurement in the free troposphere. The seasonal changes in the profile are well-captured by the model (Figures not shown). For the months not shown, the model results yield a good agreement and mostly lie within the standard deviation of the measurements for most of the locations examined.

4.2 The effect of African emissions on surface ozone

The effect of African biomass burning, biogenic VOC and anthropogenic emissions on surface ozone is shown in Figs. 3, 4 and 5 respectively. The figures show the difference between the surface ozone in the reference experiment and the experiment where each of the emission types were excluded. The 1997–2001 December–February (DJF) and June–August (JJA) seasonal average of the surface ozone is shown in the figures. DJF is the African NH burning season, while in JJA, the burning commences at the SH part of Africa. Lightning has a small impact on surface ozone, and only contributes a maximum of 1 ppbv to a small area in Africa.

During the biomass burning seasons, the local surface ozone concentration can increase by about 10–30 ppbv at the burning region (Fig. 3). This increase can be up to 50 ppbv in JJA over large parts of Democratic Republic of Congo and Angola. In DJF, there is a significant concentration of ozone over the equatorial Atlantic, reaching farther to northeastern part of Brazil. About 1–2 ppbv surface ozone produced by African biomass burning emissions in JJA as well as September to November (SON), cover most of the southern Atlantic, the Indian and the Pacific oceans.

Biogenic VOCs contribution to surface ozone concentration over Africa is lower than that contributed by biomass burning emissions (Fig. 4). The maximum contribution is about 20 ppbv. They show less seasonal variation than biomass burning (which is tied to the dry seasons at both hemispheres) because of the constant emissions from the evergreen tropical forests, which constitute the dominant source. Similar to the effect of biomass burning, African biogenic VOC emissions also contribute about 1–2 ppbv to most of the SH ocean surface, but in all seasons.

The surface ozone produced by African anthropogenic emissions (Fig. 5) shows that

Nigeria, South-Africa and Egypt are the major countries affected by anthropogenic emissions (up to 10 ppbv). This corresponds with the relatively high contribution of these countries to the anthropogenic emissions.

The relative importance of biomass burning and biogenic VOC emissions on the surface ozone over Africa depends on the season. During the burning periods of DJF and JJA, biomass burning is the most important emission category affecting the African air-quality. Apart from these two seasons, biogenic VOC emissions yield the largest contribution to the surface ozone concentration over Africa.

4.3 The contribution of African emissions to tropospheric ozone burden

The estimates of the TOB in the reference experiment for various world regions are shown in column 7 of Table 3. For the tropospheric calculation, we assume the tropopause is at 200 hPa. Our estimate of 29 Tg over Africa is close to the value of the 26 Tg reported by Marufu et al. (2000) using the Tracer Model version 3 (TM3).

The contribution of each of the African emissions to the regional and global TOB is shown in column 2 through 6 of Table 3. African biomass burning, biogenic VOC, lightning and anthropogenic emissions contribute about 9 Tg, 13 Tg, 8 Tg and 4 Tg respectively, to the global TOB. Over Africa itself, the contribution of each of these emission types is only 2.4 Tg, 2.2 Tg, 1.4 Tg and 0.8 Tg respectively. This indicates that more than 70% of the tropospheric ozone produced by photochemical reactions involving African emissions is found outside the continent due to the combination of transport of precursor species and ozone. The largest ozone enhancement is confined to the south Atlantic and Indian oceans. Our calculated value of 9 Tg of ozone due to Africa biomass burning is in good agreement with the 10 Tg suggested in a marked tracer experiment described in Marufu et al. (2000).

Over the continental regions outside Africa, the African biogenic VOC contribution to the ozone burden is two times that of the biomass burning (as shown in Table 3), making it the most important emissions source. However, this study shows that over Africa, biomass burning is the most important emission which affects African annual TOB.

African emissions have the highest impact on Latin America, southeast and south-central Asia, Oceania and the Middle east, while Canada, United States, Europe and north-central Asia are only slightly affected by African emissions (Table 3).

The vertical profile of the zonal average ozone concentration produced by African biomass burning (left column), biogenic VOC (middle column) and lightning (right column) are shown in Fig. 6. The two seasons shown for each emission source are those with the maximum impact of each of the emission types. These are DJF and JJA for biomass burning, and MAM and SON for biogenic VOC and lightning emissions. The plots show 5-year averages. The impact of African lightning emission on ozone production is highest at the middle to the upper troposphere (as shown in the right column of Fig. 6).

A striking feature in Fig. 6 (middle column) is that although the biogenic VOC emissions are released into the troposphere at the top of the vegetation canopy, relatively high ozone is seen in the upper troposphere (UT) (between 300 hPa and 100 hPa). This may be due to the combined effect of strong convective activity in the emissions main source regions (Collins et al., 1999; Lawrence et al., 2003; von Kuhlmann et al., 2004) and the transport of biogenic VOCs with relatively long chemical lifetime, such as methanol (Tie et al., 2003). In order to estimate the direct contribution of African biogenic CH_3OH, isoprene and terpene emissions to these high concentrations, we performed 3 additional sensitivity experiments for 1 year after a spin-up period of 6 months. In each of these experiments, we exclude only one of these emissions, respectively. Together, these emissions account for 96% of the biogenic VOCs used for this study. The results show that African biogenic CH_3OH and isoprene emissions contribute a maximum of 15% and 65% respectively to the UT ozone concentration produced by African biogenic VOCs, while terpenes yield a negligible contribution to the ozone enhancement. Therefore, the net effect of the convective transport of biogenic methanol and isoprene, and their reaction products increases the UT ozone (Tie et al., 2003; Doherty et al., 2005).

ACPD
6, 5797–5838, 2006

EGU

4.4 Seasonal variation of the contribution of African emissions to the regional and global tropospheric ozone burden

In this section, we will discuss the seasonality of the contributions of African emissions to TOB. We focus on Africa and global TOB, and the TOB of other world regions.

In Fig. 7a, the seasonal variation of the impact of African emissions on the TOB over Africa is shown. The seasonal variation of the tropospheric ozone burden produced by African biomass burning emissions (red line) shows two peaks. The first peak occurs between December and February, while the second peak occurs in July, with a spread from June to September. This seasonality shows a high correlation with biomass burning emissions (r=0.85, 0.88 and 0.93 for biomass burning NMHC, CO and NO_x respectively), reflecting the DJF and JJA burning seasons in the NH and SH parts of Africa, respectively. During these peaks, African biomass burning contributes up to 3.3 Tg in January and 2.8 Tg in July to the African TOB.

The seasonal variation in African TOB contributed by African biogenic VOC emissions also show a peak in May and June (green line in Fig. 7a) reaching 2.6 Tg. Lightning emissions over Africa yield a maximum contribution to the ozone production over the continent in two major seasons: March through May, and September to October; contributing a maximum of 1.6 Tg and 1.8 Tg respectively (blue line in Fig. 7a).

The largest contribution of the African emissions to the TOB over Africa clearly depends on the seasons. Emissions from biomass burning have the highest contribution during the burning seasons in November through March and July through September. Outside these periods, biogenic VOC emissions have the highest contribution to the TOB over Africa.

When the TOB produced by biogenic CO, H_2 and soil NO_x emissions is added to the TOB contributed by biogenic VOCs emissions, this combined natural emissions generated TOB show the highest contribution to the African TOB throughout the year, except in January and February, with an annual mean of about 3.4 Tg (Table 4).

As shown in Fig. 7b, biogenic VOC emissions clearly dominate the contribution to

ACPD
6, 5797–5838, 2006

EGU

global TOB in all seasons. The two maximum contributions occur in May and December, with a value 14.6 Tg and 14.5 Tg respectively. The highest isoprene emissions over Africa occur in April and October, while those of terpenes occur in May and October.

The seasonal variation of the global TOB produced by African biomass burning (red line in Fig. 7b) shows two peaks in December through February and in September. The September peak is connected with the impact of the SH part of Africa biomass burning emissions on the net ozone production over Australia and Latin America (see discussions on Fig. 8 in the paragraphs below). The maximum values are 10.5 Tg and 11.2 Tg, in February and September respectively. African lightning emissions yield their maximum contribution to global TOB in April and October. During these months, the contributions can be up to 8.8 Tg and 9.6 Tg, respectively.

As shown by the black lines in Fig. 7, the TOB produced by African anthropogenic emissions show a small seasonal variation.

Figure 8 shows the seasonal variation in the contribution of African biomass burning, biogenic VOC, lightning and anthropogenic emissions to the TOB in various world regions. The Figure shows that Latin America, southeast and south-central Asia, Oceania, and the Middle East experience the largest impact of African emissions.

African biomass burning emissions contribute more than 0.2 Tg to the TOB of Latin America, Middle east, United States and Canada, southeast and south-central Asia, and East Asia from December until March. Burning activity at this time of the year is mostly confined to African region north of the equator. The maximum impact during this period depends on the region. For example, in Latin America, the maximum of about 0.56 Tg occurs in January, whereas in the Middle East, southeast and south-central Asia, and eastern Asia, the maximums occur in February with a value of 0.38 Tg, 0.55 Tg and 0.25 Tg respectively. In the United States, the impact reaches a maximum in March with a value of 0.31 Tg. In June through October, the biomass burning of the SH part of Africa also contributed more than 0.2 Tg to the TOB of Latin America and Oceania, with a maximum contribution of up to 0.43 Tg in Latin America and 0.48 Tg in Oceania in September (see Fig. 8a).

ACPD
6, 5797–5838, 2006

EGU

Therefore, Latin America experiences a tropospheric ozone enhancement throughout the year except from April to early June due to African biomass burning. However, the tropospheric ozone enhancement over Australia is only due to the biomass burning of the southern hemispheric part of Africa. As we have mentioned before, the tropospheric ozone enhancement in Europe and north-central Asia due to biomass burning emissions in Africa is small and remains less than 0.2 Tg throughout the whole year.

Figure 8b shows that the maximum tropospheric ozone enhancement caused by the biogenic VOC emissions varies from region to region. The tropospheric ozone enhancement reaches the maximum in June over Latin America and Oceania, in May over the Middle East, in January–December over North America and north-central Asia. Other parts of Asia (east, southeast and south-central Asia) experience the maximum enhancement of tropospheric ozone from March until May and November. The maximum contribution of African biogenic VOC to the TOB of the four Asian regions ranges from 0.26 Tg in north-central Asia to 0.65 Tg in southeast and south-central Asia. Over United States and Canada, Middle East, Oceania and Latin America, the largest contribution to the TOB by African biogenic VOC can be up to 0.44 Tg, 0.46 Tg, 0.49 Tg and 0.85 Tg respectively. Again, the impact of biogenic VOC on the TOB of Europe and north-central Asia is less than 0.3 Tg throughout the year.

The effect of African lightning emissions on the TOB also depends on the region. The largest effect occurs during two distinct periods of March–June and October–November over southeast and south-central Asia, Oceania, the Middle East and East Asia. Over Latin America, the United States and Canada however, the maximum effect of African lightning on tropospheric ozone occurs in June–September, and November–December respectively. Again the African lightning contribution to TOB over Europe is less than 0.15 Tg, while that over north-central Asia is not more than 0.13 Tg in all seasons. The highest contribution of 0.24 Tg is found over United States and Canada in November. A maximum value of 0.23 Tg and 0.62 Tg is found over east and southeast and south-central Asia respectively in October. Over the Middle east and Oceania, the maximum values are 0.39 Tg and 0.36 Tg respectively in October.

The seasonal variation of the effect of African biogenic VOCs and lightning NO_x emissions on the tropospheric ozone over these world regions is determined by the transport pathways out of Africa in the middle and upper troposphere. The seasonal variation of the spatial distribution of lightning emissions (figures not shown) shows that the emission occurs at the southern hemispheric part of Africa in DJF. In March and April, the region where lightning emissions occur gradually shifts northward, and stays over part of western, eastern and central Africa from May until September. The southward shift in the lightning emissions concludes the cycle in October and November. The seasonality of the spatial distribution of the tropospheric ozone column produced by African lightning (Fig. 9) shows a similar spatial distribution over Africa.

Figure 8d shows the seasonality of the contribution of the African anthropogenic emissions to the TOB of different regions of the world. It reveals that over all the regions, except Latin America, the maximum impact occurs in March–April and October–November. The maximum impact occurs in June–August in Latin America. The seasonality observed in Fig. 8d cannot be explained by the seasonal variation of the anthropogenic emissions, because they are almost constant throughout the year. Therefore, we attribute the seasonal variation in the ozone burden to seasonally changing transport patterns. For all the regions, the maximum contribution of the African anthropogenic emissions to the TOB is less than 0.21 Tg.

4.5 Inter-annual variability

Previous studies on the effect of African emissions on tropospheric ozone have always focused on one specific meteorological year. The authors are not aware of any study conducted over several years. Here we investigate the impact of changes in meteorology by analysing the inter-annual variability in our 5-years simulations. All emissions were held constant over the 5-years, but lightning emissions vary according to changes in convective activity.

We give the inter-annual variability calculated as the average deviation from the mean results we presented in previous sections (Table 5). The maximum inter-annual

variability of about 15% is calculated for southeast Asia, while the minimum inter-annual variability of about 3% is recorded over Africa. Globally, the variability is about 3.0%, 2.3%, 5.7% and 1.9% for global tropospheric ozone burden generated by African biomass burning, biogenic VOC, lightning and anthropogenic emissions respectively. So, variability of the tropospheric ozone burden produced by African emissions over Africa is small, but not over Southeast Asia, due to a large variation in transport.

In a separate study (Aghedo et al., 2005) with the MEGAN module of MOZECH, we calculated the global inter-annual variability of isoprene and terpene emissions to be about 2.5% and 2.0% respectively; and over Africa, the values are 3.3% and 2.8% respectively. For lightning emissions, the inter-annual variability is about 3% globally and about 4.6% over Africa.

4.6 Uncertainties

Simulations of the global tropospheric ozone budget are still rather uncertain; nevertheless, most models show rather good consistency in simulating the response to emission changes (Stevenson et al., 2006). There are large uncertainties in emission estimates, and these uncertainties will influence our results both in terms of absolute values and with respect to the relative importance of emission source types. While we cannot give a thorough discussion of the uncertainties here, we will at least discuss the potential impact of emission uncertainties on our ozone budget calculations assuming a linear response for simplicity.

African biomass burning emissions are uncertain by about a factor of 2 (Schultz et al., 2006)[1]. Some of this uncertainty may be related to inter-annual variability of these emissions (e.g see, Barbosa et al., 1999), but since we do not take this variability into account in our model simulations, we can regard it as a source of uncertainty here. Thus the contribution of African biomass burning emissions to global tropospheric ozone burden could range from 4 Tg (O_3) to 18 Tg (O_3).

The uncertainty of global isoprene emissions reported by Guenther et al. (2006) is about a factor of 3, and about the same uncertainty factor is noted for global methanol

emissions in Tie et al. (2003). However, the uncertainty of the biogenic VOC emissions e.g. isoprene, for a specific location and time in Africa could be up to a factor of 5 (Guenther et al., 1999). Hence the contribution of African biogenic VOC emissions to global tropospheric ozone burden could be within the range of 4 Tg (O_3) and 40 Tg (O_3).

The uncertainty of global lightning emissions has been briefly discussed in Sect. 1. While there is a consistent growth of the consensus that the upper limit estimate of 20 Tg (N) yr^{-1} (Lawrence et al., 1995) is likely too high, there still remains at least an uncertainty of a factor of 3. Our estimate of 2.7 Tg (N) yr^{-1} is closer to the lower limit. We therefore estimate the global tropospheric ozone burden related to African lightning NO_x source as 6 Tg (O_3)–30 Tg (O_3) for global lightning NO_x ranging from 2 Tg (N) yr^{-1}–10 Tg (N) yr^{-1}.

Anthropogenic emissions are also uncertain by at least 30%, but uncertainties may be much larger, in particular for domestic burning. We estimate that the impact of African anthropogenic emissions on the global TOB may be between 3–6 Tg (O_3) yr^{-1}.

5 Summary and conclusions

We have discussed the effect of African emissions, namely: biomass burning, biogenic VOCs, lightning and anthropogenic on the tropospheric ozone over Africa and in other regions of the world, using the new 3-D global atmospheric chemistry model, MOZECH. We gave an overall description of the model and presented some validation results of the comparison with MOZAIC aircraft data. Generally MOZECH captures the vertical and spatial distribution of the tropospheric ozone.

We have shown that African biomass burning emissions are responsible for African regional surface ozone enhancement of 10–30 ppbv close to the burning regions. The surface ozone enhancement can be up to 50 ppbv over large parts of central Africa (Democratic republic of Congo, Congo and Angola) during JJA biomass burning season. Biogenic VOC emissions also yield a contribution of 5–20 ppbv on the surface ozone over Africa. Lightning is shown to have an insignificant impact on surface ozone,

but provides the second largest impact on the middle to the upper tropospheric ozone concentration, next to biogenic VOC emissions. The relative importance of biomass burning and biogenic VOC emissions on the surface ozone concentration over Africa is highly dependent on the season. During the burning periods of December–February and June–September, biomass burning emissions have the maximum contribution to the African surface ozone concentration. Apart from these two seasons, biogenic VOC emissions yield the largest contribution to the surface ozone concentration over Africa.

Biogenic VOC, biomass burning, lightning and anthropogenic emissions over Africa have been shown to contribute 13 Tg (4–40 Tg), 9 Tg (4–18 Tg), 8 Tg (6–30 Tg), and 4 Tg (3–6 Tg) respectively to the global tropospheric ozone burden. The contribution of total African biogenic emissions (i.e. biogenic VOC, CO, H_2 and soil NO_x) to the global tropospheric ozone burden is up to 17 Tg. Biogenic emissions over Africa have the largest contribution to the global tropospheric ozone burden, followed by biomass burning and lightning emissions.

We have also estimated the impact of biomass burning, biogenic VOC, lightning and anthropogenic emissions on the tropospheric ozone burden of various world regions. We found that for all the emissions categories, Latin America experiences the highest impact of African emissions, followed by southeast and south-central Asia, Oceania, and the Middle East. This is in effect due to the proximity of these regions to Africa and their positions are generally downwind of the two trade winds crossing Africa. For example our simulations show that it will take only approximately ten days for atmospheric species emitted or produced in West Africa to get to Brazil in South America. The tropospheric ozone over Canada, the United States, Russia, Mongolia and Europe are only slightly affected by African emissions.

Acknowledgements. This work is sponsored by the ZEIT foundation. We acknowledge the MOZAIC programme, made possible by the support of the European Commission, Airbus, CNRS-France, FZJ-Germany and the airlines (Lufthansa, Air France, Austrian and former Sabena, who carry the MOZAIC instrumentation free of charge since the commencement of the campaign in 1994). We are grateful to M. Esch and U. Schulzweida for their technical assistance. We also appreciate the valuable comments of J. Feichter and M. A. Pfeffer. The model

runs were performed on the NEC SX-6 computer at the German Climate Computing Centre ("Deutsches Klimarechenzentrum" (DKRZ)).

References

Aghedo, A. M., Schultz, M. G., Sebastian, R., Guenther A., and Wiedinmyer, C.: Climate Impact on Biogenic VOC emissions, poster EGU05-A-03390, EGU General Assebly, Vienna, Austria, April 2005. 5801, 5815

Amann, M., Bertok, I., Cofala, J., Gyarfas, F., Heyes, C., Klimont, Z., Makowski, M., Schöpp, W., and Syri, S.: Cost-effective Control of Acidification and Ground-Level Ozone, Seventh Interim Report, International Institute for Applied Systems Analysis (IIASA), Laxenburg, Austria, 1999. 5805

Andreae, M. O.: The influence of tropical biomass burning on climate and the atmospheric environment, in: Biogeochemistry of Global Change: Radiatively Active Trace Gases, edited by: R. S. Oremland, 113–150, Chapman and Hall, New York, 1993. 5799

Asselin, R.: Frequency filter for time integrations, Mon. Wea. Rev., 100, 487–490, 1972. 5802

Aviation and the Global Atmosphere: A Special Report of IPCC Working Groups I and III in collaboration with the Scientific Assessment Panel to the Montreal Protocol on Substances that Deplete the Ozone Layer, edited by: Penner, J. E., Lister, D. H., Griggs, D. J., Dokken, D. J., and McFarland, M., Cambridge University Press, UK, pp. 373, 1999. 5805

Barbosa, P. M., Stroppiana, D., Grégoire, J.-M., and Pereira, J. M. C.: An assessment of vegetation fire in Africa (1981–1991): Burned area, burned biomass, and atmospheric emissions, Global Biogeo. Cycles, 13, 933–950, 1999. 5815

Brasseur, G. P, Mueller, J.-F., and Granier, C.: Atmospheric impact of NO_x emissions by subsonic aircraft: A three-dimensional model study, J. Geophys. Res., 101, 1423–1428, 1996. 5800

Collins, W. J., Stevenson, D. S., Johnson, C. E., and Derwent, R. G.: Role of convection in determining the budget of odd hydrogen in the upper troposphere, J. Geophys. Res., 104(D21), 26 927–26 942, doi:10.1029/1999JD900143, 1999. 5810

Crutzen, P. J., Heidt, L. E., Krasnec, W. H., and Seiler, W.: Biomass burning as a source of atmospheric trace gases CO, H_2, N_2O, NO, CH_3Cl and COS, Nature, 282, 253–256, 1979. 5799

Crutzen, P. J. and Andreae, M. O.: Biomass burning in the tropics: Impact on atmospheric chemistry and biogeochemical cycles, Science, 150, 1669–1678, 1990. 5799

DeCaria, A. J., Pickering, K. E., Stenchikov, G. L., Scala, J. R., Stith, J. L., Dye, J. E., Ridley, B. A., and Laroche P.: A cloud-scale model study of lightning-generated NO_x in an individual thunderstorm during STERAO-A, J. Geophys. Res., 105, 11 601–11 616, 2000. 5800

DeCaria, A. J., Pickering, K. E., Stenchikov, G. L. , and Ott, L. E.: Lightning-generated NO_x and its impact on tropospheric ozone production: A three-dimensional modeling study of a Stratosphere-Troposphere Experiment: Radiation, Aerosols and Ozone (STERAO-A) thunderstorm, J. Geophys. Res., 110, D14303, doi:10.1029/2004JD005556, 2005. 5800

Desqueyroux, H., Pujet, J. C., Prosper, M., Squinazi, F., and Momas, I.: Short-term effects of low-level air pollution on respiratory health of adults suffering from moderate to severe asthma, Environ. Res., 89, 2937, 2002 5799

Doherty, R. M., Stevenson, D. S., Collins, W. J., and Sanderson, M. G.: Influence of convective transport on tropospheric ozone and its precursors in a chemistry-climate model, Atmos. Chem. Phys., 5, 3205–3318, 2005. 5810

Fehsenfeld, F., Calvert, J., Fall, R., Goldan, P., Guenther, A. B., Hewitt, C. N, Lamb, B., Liu, S., Trainer, M., Westberg, H., and Zimmerman, P.: Emissions of volatile organic compounds from vegetation and the implications for atmospheric chemistry, Global Biogeochem. Cycles, 6(4), 389–430, 1992. 5801

Ganzeveld, L.: Surface-Atmosphere Trace Gas and Aerosol Exchanges on the Global Scale, PhD thesis, University of Utrecht, The Netherlands, 2001. 5803

Grewe, V., Brunner, D., Dameris, M., Grenfell, J. L., Hein, R., Shindell, D., and Staehelin, J.: Origin and variability of upper tropospheric nitrogen oxides and ozone at northern mid-latitudes, Atmos. Environ. 35, 3421–3433, 2001. 5803

Guenther, A., Hewitt, C. N., Erickson, D., Fall, R., Geron, C., Graedel, T., Harley, P., Klinger, L., Lerdau, M., Mckay, W. A., Pierce, T., Scholes, B., Steinbrecher, R., Tallamraju, R., Taylor, J., and Zimmerman, P. A.: Global-Model of Natural Volatile Organic-Compound Emissions, J. Geophys. Res.-Atmos., 100(D5), 8873–8892, 1995. 5801, 5805

Guenther, A., Baugh, B., Brasseur, G., Greenberg, J., Harley, P., Klinger, L., Serca, D., and Vierling, L.: Isoprene emission estimates and uncertainties for the Central African EXPRESSO study domain, J. Geophys. Res., 104(30), 625–639, 1999. 5816

Guenther, A., Karl, T., Harley, P., Wiedinmyer, C., Palmer, P. I, and Geron, C.: Estimates of global terrestrial isoprene emissions using MEGAN (Model of Emissions of Gases and

Aerosols from Nature), Atmos. Chem. Phys. Discuss., 6, 107–173, 2006. 5801, 5804, 5815
Hansen, J., Sato, M., Nazarenko, L., Ruedy, R., et al.: Climate forcings in GISS SI2000 simulations, J. Geophys. Res. 107, 4347, doi:10.1029/2001JD001143, 2002. 5799
Hoke, J. E. and Anthes, R. A.: The initialization of numerical models by a dynamic-initialization technique, Mon. Wea. Rev., 104(12), 1551–1556, 1976.
Horowitz, L. W., Walters, S., Mauzerall, D. L., Emmons, L. K., Rasch, P. J., Granier, C., Tie, X., Lamarque, J.-F., Schultz, M. G., Tyndall, G. S., Orlando, J. J., and Brasseur, G. P.: A global simulation of tropospheric ozone and related tracers: Description and evaluation of MOZART, version 2, J. Geophys. Res., 108(D24), 4784, doi:10.1029/2002JD002853, 2003. 5802, 5805
Huntrieser, H., Feigl, C., Schlager, H., Schröder, F., Gerbig, C., van Velthoven, P., Flatøy, F., Théry, C., Petzold, A., Höller, H., and Schumann, U.: Airborne measurements of NO_x, tracer species, and small particles during the European Lightning Nitrogen Oxides Experiment, J. Geophys. Res., 107(D11), 4113, doi:10.1029/2000JD000209, 2002. 5800, 5803
Jeuken, A. B. M., Siegmund, P. C., Heijboer, L. C., Feichter, J., and Bengtson, L.: On the potential of assimilating meteorological analysis in a climate model for the purpose of model validation, J. Geophys. Res., 101, 16 939–16 950, 1996.
Kesselmeier, J. and Staudt, M.: Biogenic volatile organic compounds (VOC): An overview on emission, physiology and ecology, J. Atmos. Chem., 33, 23–88, 1999. 5800, 5801
Lamarque, J.-F., Brasseur, G. P, Hess, P. G., and Mueller, J.-F.: Three dimensional study of the relative contributions of the different nitrogen sources in the troposphere, J. Geophys. Res., 101, 22 955–22 968, 1996. 5800
Lawrence, M. G., Chameides, W. L., Kasibhatla, P, S., Levy II, H., and Moxim, W.: Lightning and atmospheric chemistry: The rate of atmospheric NO production, in: Handbook of Atmospheric Electrodynamics, edited by: Volland, H., Vol. I, CRC Press, Inc., Boca Raton, 189–202, 1995. 5800, 5816
Lawrence, M. G., von Kuhlmann, R., and Salzmann, M.: The balance of effects of deep convective mixing on tropospheric ozone, Geophys. Res. Lett., 30, 18, 1940, doi:10.1029/2003GL017644, 2003. 5810
Lin, S.-J. and Rood, R. B.: Multidimensional Flux-Form Semi-Lagrangian Scheme. Mon. Wea. Rev., 124, 2046–2070, 1996. 5803
Liu, S. C., Trainer, M., Fehsenfeld, F. C., Parrish, D. D., Williams, E. J. , Fahey, D. W., Huebler, G., and Murphy, P. C.: Ozone production in the rural troposphere and the implications for

regional and global ozone distributions, J. Geophys. Res., 92, 4191–4207, 1987. 5800
Marenco, A., Medale, J. C., and Prieur, S.: Study of tropospheric ozone in the tropical belt (Africa, America) from STRATOZ and TROPOZ campaigns, Atmos. Environn., Ser. A, 24, 2823–2843, 1990. 5799
Marenco, A., Thouret, V., Nédélec, P., Smit, H., Helten, M., Kley, D., Karcher, F., Simon, P., Law, K., Pyle, J., Poschmann, G., Von Wrede, R., Hume, C., and Cook, T.: Measurement of ozone and water vapor by Airbus in-service aircraft: The MOZAIC airborne program, An overview, J. Geophys. Res.-Atmospheres, 103(D19), 25 631–25 642, 1998. 5807
Martin, R. V., Jacob, D. J., Logan, J. A., Bey, I., Yantosca, R. M., Staudt, A. C., Li, Q., Fiore, A. M., Duncan, B. N., and Liuiu, H., Ginoux, P., and Thouret, V.: Interpretation of TOMS observations of tropical tropospheric ozone with a global model and in situ observations, J. Geophys. Res., 107(D18), 4351, doi:10.1029/2001JD001480, 2002. 5800
Marufu, L., Ludwig, J., Andreae, M. O.,Lelieveld J., and Helas G.: Spatial and temporal variation in biofuel consumption rates and patterns in Zimbabwe: Implications for atmospheric trace gas emissions, Biomass Bioenergy, 16, 311–332, 1999.
Marufu, L., Dentener, F., Lelieveld J., Andreae, M. O., and Helas G.: Photochemistry of the African troposphere: Influence of biomass-burning emissions, J. Geophys. Res., 105, 14 513–14 530, 2000. 5799, 5809
Mauzerall, D. L. and Wang, X. P.: Protecting agricultural crops from the effects of tropospheric ozone exposure: Reconciling science and standard setting in the United States, Europe, and Asia, Ann. Rev. Energy Environ., 26, 237–268, 2001. 5799
Mesinger, F. and Arakawa, A.: Numerical methods used in atmospheric models, Global Atmospheric Research Programme (GARP) Publication Series 17, World Meteorological Organisation, 1976. 5803
Mortimer, K. M., Neas, L. M., Dockery, D. W., Redline, S., and Tager, I. B.: The effect of air pollution on inner-city children with asthma, Eur Respiratory J., 19, 699–705, 2002. 5799
Nordeng, T. E.: Extended versions of the convective parameterization scheme at ECMWF and their impact on the mean and transient activity of the model in the tropics. Technical memorandum No. 206, European Centre for Medium-range Weather Forecasts (ECMWF), Reading, United Kingdom, 1994. 5803
Oksanen, E., and T. Holopainen: Responses of two birch (Betula pendula Roth) clones to different ozone profiles with similar AOT40 exposure, Atm. Environ., 35, 5245–5254, 2001. 5799

Olivier, J., Bouwman, A., Berdowski, J., Bloos, J., Visschedijk, A., van der Mass, C., and Zandveld, P.: Sectoral emission inventories of greenhouse gases for 1990 on a per country basis as well as on 1×1 degrees, Environ. Sci. Policy, 2, 241–263, 1999. 5805

Peden, D. B.: Air pollution in asthma: effect of pollutants on airway inflammation, Annals Allergy Asthma and Immunology, 87, 1217, 2001. 5799

Pickering, K. E., Thompson, A. M., Dickerson, R. R., Luke, W. T., McNamara, D. P., Greenberg, J., and Zimmerman, P. R.: Model calculations of tropospheric ozone production potential following observed convective events, J. Geophys. Res., 95, 14 049–14 062, 1990. 5800

Pickering, K. E., Thompson, A. M., Wang. Y., Tao, W., McNamara, D. P., Kirchhoff, V. W. J. H., Heikes, B. G., Sachse, G. W., Bradshaw, J. D., Gregory, G. L., and Blake, D. R.: Convective transport of biomass burning emissions over Brazil during TRACE-A, J. Geophys. Res., 101, 23 993–24 012, 1996. 5800

Pickering, K. E., Wang, Y., Tao, W., Price, C., and Müller, J.: Vertical distributions of lightning NOx for use in regional and global chemical transport models, J. Geophys. Res., 103(D23), 31 203–31 216 ,1998. 5800, 5803

Price, C., Penner, J., and Prather, M.: NO_x from lightning: 1. Global distribution based on lightning physics, J. Geophys. Res., 102, 5929–5941, 1997. 5800

Randerson, J. T., Kasibhatla, P. S., Kasischke, E. S., Hyer, E. J., Giglio, L., Collatz, G. J., and van der Werf, G. R.: Global Fire Emissions Database (GFED), Version 1. Data set. Available on-line http://daac.ornl.gov/ from Oak Ridge National Laboratory Distributed Active Archive Center, Oak Ridge, Tennessee, USA, 2005. 5805

Ridley, B. A., Dye, J. E., Walega, J. G., Zheng, J., Grahek, F. E., and Rison, W.: On the production of active nitrogen by thunderstorms over New Mexico, J. Geophys. Res., 101, 20 985–21 005, 1996. 5800

Robert, A. J., Henderson, J., and Turnbull, C.: An implicit time integration scheme for baroclinic models in the atmosphere, Mon Wea. Rev., 100, 329–335, 1972. 5802

Robert, A. J.: A stable numerical integration scheme for the primitive meteorological equations, Atmos. Ocean, 19, 35–46, 1981. 5802

Robert, A. J.: A semi-Lagrangian and semi-implicit numerical integration fscheme for the primitive meteorological equations, J. Met. Soc. Japan, 60, 319–325, 1982. 5802

Roeckner, E., Bäuml, G., Bonaventura, L., Brokopf, R., Esch, M., Giorgetta, M., Hagemann, S., Kirchner, I., Kornblueh, L., Manzini, E., Rhodin, A., Schlese, U., Schulzweida, U., and Tompkins, A.: The atmospheric general circulation model ECHAM5, part I: Model description, Max

Planck Institute for Meteorology, Report No. 349, 2003. 5801, 5803
Roeckner, E., Brokopf, R., Esch, M., Giorgetta, M., Hagemann, S., Kornblueh, L., Manzini, E., Schlese, U., and Schulzweida, U.: Sensitivity of simulated climate to horizontal and vertical resolution in the ECHAM5 atmosphere model, in press, J. Climate, 2006. 5802, 5805
Schultz, M. G. and Bey, I.: Numerical modeling of long-range pollution transport, Chp. 8, in: Intercontinental Transport of Air Pollution, edited by: Stohl, A., Springer, New York, 2004.
Seinfeld, J. H. and Pandis, S. N.: Atmospheric Chemistry and Physics: From Air pollution to Climate change, John Wiley, United States of America, 1998. 5803
Simmons, A. J and Burridge, D. M.: An energy and angular-momentum conserving vertical finite difference scheme and hybrid vertical coordinates, Mon. Wea. Rev., 109, 758–766, 1981. 5802
Stevenson, D. S., Dentener, F. J., Schultz, M. G., Ellingsen, K., van Noije, T. P. C., et al.: Multi-model ensemble simulations of present-day and near-future tropospheric ozone, J. Geophys. Res., 111(D8), D08301, doi:10.1029/2005JD006338, 2006. 5804, 5806, 5815
Stier, P., Feichter, J., Kinne, S., Kloster, S., Vignati, E., Wilson, J., Ganzeveld, L., Tegen, I., Werner, M., Balkanski, Y., Schulz, M., Boucher, O., Minikin, A., and Petzold, A.: The aerosol-climate model ECHAM5-HAM, Atmos. Chem. Phys., 5, 1125–1156, 2005. 5803
Thouret, V., Marenco, A., Logan, J. A., Nédélec, P., and Grouhel, C.: Comparison of ozone measurements from the MOZAIC airborne program and the ozone sounding network at eight locations, J. Geophys. Res., 103(D19), 25 695–25 720, 1998a. 5807
Thouret, V., Marenco, A., Nédélec, P., and Grouhel, C.: Ozone climatologies at 9–12 km altitude as seen by the MOZAIC airborne program between September 1994 and August 1996, J. Geophys. Res., 103(D19), 25 653–25 680, doi:10.1029/98JD01807, 1998b. 5807
Thouret, V. , Cammas, J.-P., Sauvage, B., Athier, G., Zbinden, R., Nédélec, P., Simon, P. and Karcher, F.: Tropopause referenced ozone climatology and inter-annual variability (1994–2003) from the MOZAIC programme, Atmos. Chem. Phys., 6, 1033–1051, 2006. 5807
Tie, X., Zhang, R. , Brasseur, G., Emmons, L., and Lei, W.: Effects of lightning on reactive nitrogen and nitrogen reservoir species in the atmosphere, J. Geophys. Res., 106, 3167–3178, 2001. 5800
Tie, X., Guenther, A., and Holland, E.: Biogenic methanol and its impact on tropospheric oxidants, Geophys. Res. Lett., 30(17), 1881, doi:10.1029/2003GL017167, 2003. 5801, 5810, 5816
Tiedtke, M.: A comprehensive mass flux scheme for cumulus parameterization in large-scale

models, Mon. Wea. Rev., 117, 1779–1800, 1989. 5803
von Kuhlmann, R., Lawrence, M. G., Pöschl, U., and Crutzen, P. J.: Sensitivities in global scale 25 modeling of isoprene, Atmos. Chem. Phys., 4, 117, 2004. 5810
Wang, W. C., Pinto, J. P., and Yung, Y. L.: Climatic effect due to halogenated compounds in the Earth's atmosphere, J. Atmos. Sci., 37, 333–338, 1980. 5799
Wang, K.-Y. and Shallcross, D. E: Modelling terrestrial biogenic isoprene fluxes and their potential impact on global chemical species using a coupled LSM-CTM model, Atmos. Environ., 34, 2909–2925, 2000. 5801
Zbinden, R. M. , Cammas, J.-P., Thouret, V., Nédélec, P., Karcher, F. and Simon, P.: Mid-latitude tropospheric ozone columns from the MOZAIC program: climatology and interannual variability Atmospheric Chemistry and Physics, 6, 1053- 1073, 2006. 5807

Table 1. Global trace gas emissions by source used in this study.

Source	CO (Tg (C)/yr)	NMHC (Tg (C)/yr)	NO_x (Tg (N)/yr)
Industrial	201	66	28.0
Biomass burning	217	19	10.0
Biogenic	69	756	8.0
Lightning	–	–	2.7
Aircraft	–	–	0.7
Ocean	9	4	–
Total	496	845	49.4

ACPD
6, 5797–5838, 2006

EGU

Table 2. African trace gas emissions by source used in this study.

Source	CO (Tg (C)/yr)	NMHC (Tg (C)/yr)	NO_x (Tg (N)/yr)
Industrial	32	9	1.40
Biomass burning	93	8	4.60
Biogenic	14	186	2.40
Lightning	–	–	0.70
Aircraft	–	–	0.03
Total	139	203	9.13

ACPD
6, 5797–5838, 2006

EGU

Table 3. African emissions contribution to the 1997–2001 average tropospheric ozone burden ($Tg\,O_3$) of various world regions.

Region	Biomass burning	Biogenic VOC	Lightning	Anthropogenic	Biogenic CO, H_2 and soil NO_x	Tropospheric O_3 burden
Africa	2.35	2.20	1.41	0.80	1.22	29
Oceania[a]	0.24	0.40	0.28	0.12	0.11	9
United States and Canada	0.15	0.30	0.15	0.11	0.07	25
Latin America[b]	0.38	0.68	0.43	0.18	0.18	21
Europe	0.10	0.21	0.10	0.09	0.05	17
East Asia[c]	0.12	0.24	0.14	0.09	0.06	12
Southeast and south central Asia[d]	0.29	0.50	0.37	0.14	0.14	15
North-central Asia[e]	0.09	0.18	0.08	0.09	0.04	19
Middle East[f]	0.19	0.36	0.24	0.17	0.13	12
Global	9.00	13.30	8.06	4.36	4.17	378

[a] Australia, New Zealand, Fijis, French Polynesia, Guam, New Caledonia, Niue, Samoa and Vanuatu.
[b] South America, Mexico and the Caribbean Islands.
[c] China, Hong Kong, Japan, Democratic peoples Republic of Korea, Republic of Korea, Macau and Taiwan.
[d] Southeast and south-central Asia consist of Cambodia, East Timor, Laos, Vietnam, Indonesia, Brunei, Malaysia, Myanmar, Papau New Guinea, Philippines, Singapore, Thailand, India, Pakistan, Bangladesh, Sri-Lanka, Nepal, Maldives, Kashmir, Bhutan and the eastern Afghanistan.
[e] Russia Federation and Mongolia.
[f] Middle East countries include the western part of Afghanistan, Bahrain, Cyprus, Gaza strip, Iran, Iraq, Israel, Jordan, Kazakhstan, Kuwait, Kyrgyzstan, Lebanon, Oman, Pakistan, Qatar, Saudi Arabia, Syrian Arab republic, Turkey, Turkmenistan, United Arab Emirates, Uzbekistan, West Bank and Yemen.

ACPD
6, 5797–5838, 2006

Table 4. Comparison of African tropospheric ozone burden ($Tg\,O_3$) due to African biomass burning and natural emissions (sum of biogenic VOC, CO, H_2 and soil emissions). Values are 1997–2001 averages.

	Jan.	Feb.	March	April	May	June	July	Aug.	Sept.	Oct.	Nov.	Dec.
Biomass burning	3.26	3.06	1.82	1.00	1.38	2.45	2.84	2.73	2.47	1.79	2.29	3.14
Natural emissions	2.94	3.03	3.48	3.63	4.04	3.85	3.49	3.34	3.34	3.37	3.35	3.14

Table 5. Inter-annual variability of the tropospheric ozone burden produced by each of the African emission categories. The entries show the average deviation (%) for the respective regions.

Region	Biomass burning	Biogenic VOC	Lightning	Anthropogenic
Africa	2.4	2.7	4.5	2.0
Oceania	4.2	2.9	6.0	1.7
United States and Canada	7.2	3.6	6.0	4.4
Latin America	4.0	3.2	6.5	2.8
Western Europe	5.4	2.7	5.0	4.7
Eastern Europe	5.9	3.4	5.9	7.4
East Asia	6.7	3.1	6.1	3.6
Southeast Asia	16.0	11.0	18.5	11.0
South-Central Asia	6.6	3.2	4.4	1.6
North-central Asia	7.3	3.8	5.4	4.8
Middle East	6.6	4.7	4.3	0.8
Global	3.0	2.3	5.7	1.9

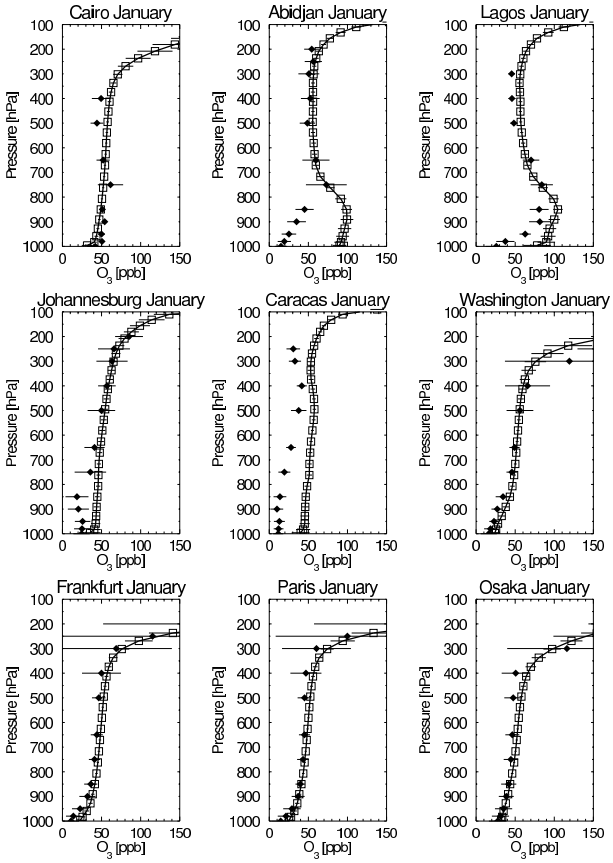

Fig. 1. The comparison of 1997–2001 monthly mean model simulated (squares) and 1997–2002 monthly mean MOZAIC (diamonds) ozone vertical profiles for Cairo, Abidjan, Lagos, Johannesburg, Caracas, Washington DC, Frankfurt, Paris and Osaka in January. The horizontal lines indicate $\pm 1\sigma$ standard deviation.

ACPD
6, 5797–5838, 2006

EGU

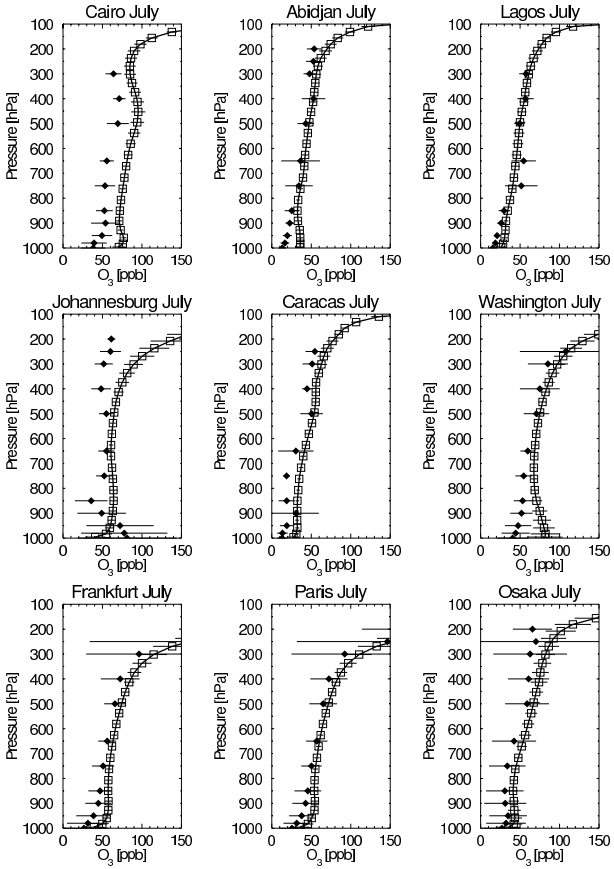

Fig. 2. Same as Fig. 1 but for July.

ACPD
6, 5797–5838, 2006

EGU

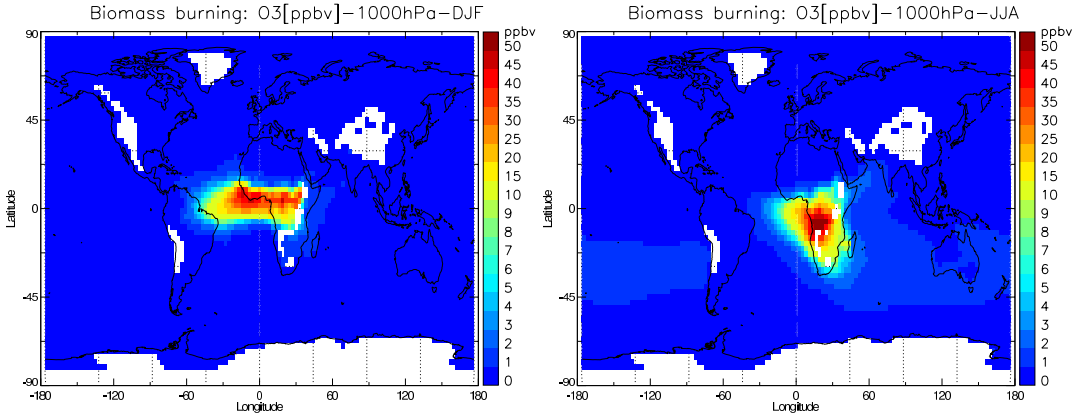

Fig. 3. 1997–2001 DJF and JJA seasonal average of the surface ozone concentration contributed by African biomass burning. The figures show the difference between the surface ozone in the reference experiment and the experiment where biomass burning emissions are excluded.

ACPD
6, 5797–5838, 2006

EGU

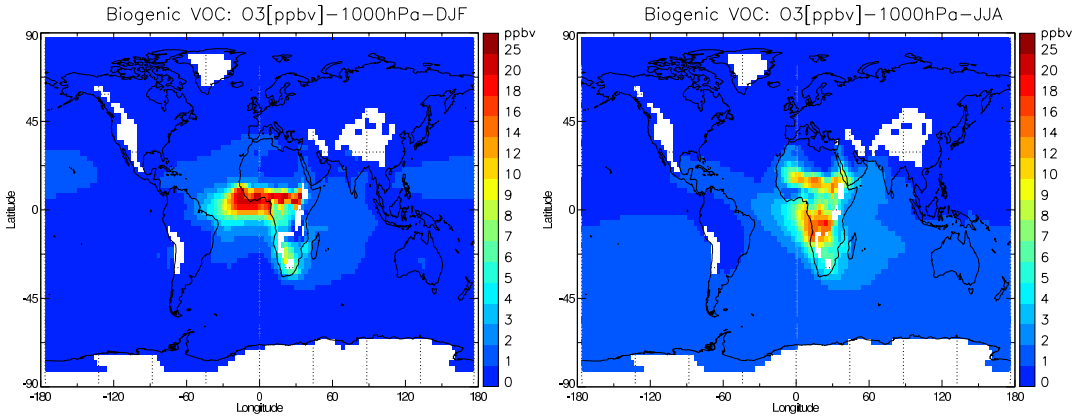

Fig. 4. 1997–2001 DJF and JJA seasonal average of the surface ozone concentration contributed by African biogenic VOC emissions. The figures show the difference between the surface ozone in the reference experiment and the experiment where biogenic VOC emissions are excluded. Note that the scale is reduced from that of Fig. 3.

ACPD
6, 5797–5838, 2006

EGU

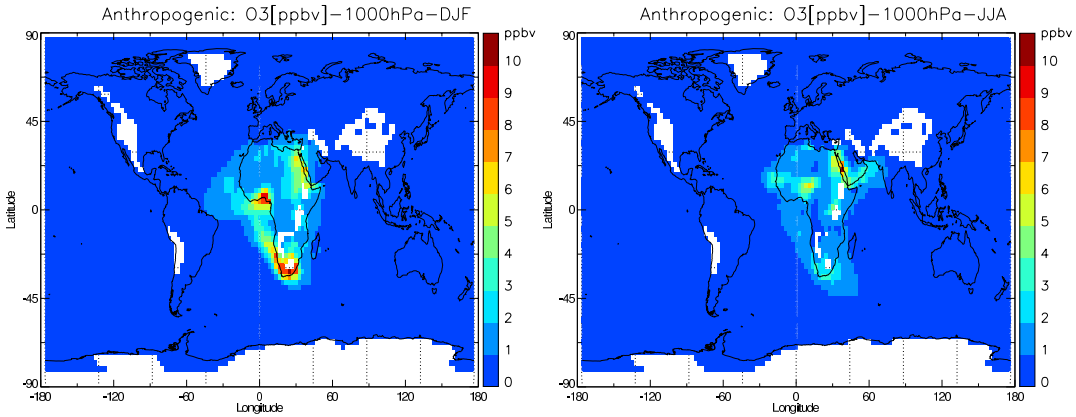

Fig. 5. 1997–2001 DJF and JJA seasonal average of surface ozone concentration contributed by African anthropogenic emissions. The figures show the difference between the surface ozone in the reference experiment and the experiment where anthropogenic emissions are excluded. Note that the scale is further reduced from those of Figs. 3 and 4.

ACPD
6, 5797–5838, 2006

EGU

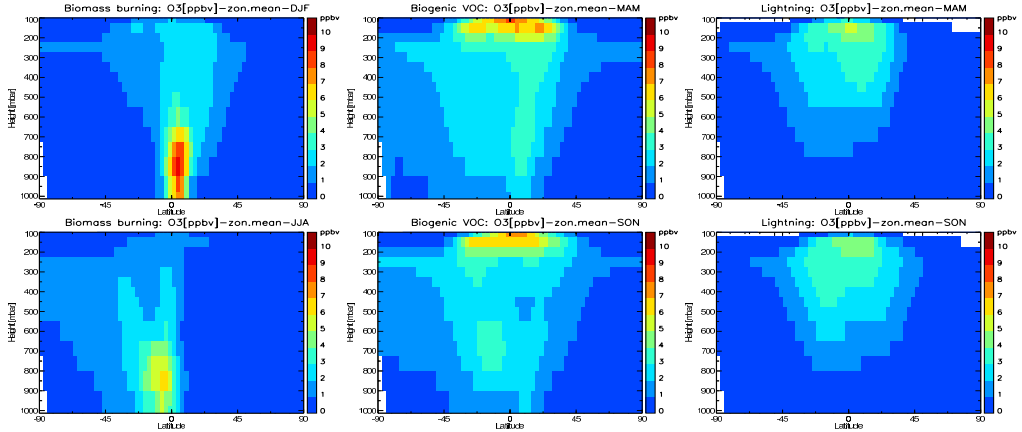

Fig. 6. 1997–2001 zonal average of the ozone concentration (ppbv) produced by African biomass burning (left column), biogenic VOC (middle column) and lightning (right column) emissions. The seasons with highest ozone enhancement are shown. These are DJF and JJA for Biomass burning; and MAM and SON for biogenic VOC and lightning emissions.

ACPD
6, 5797–5838, 2006

EGU

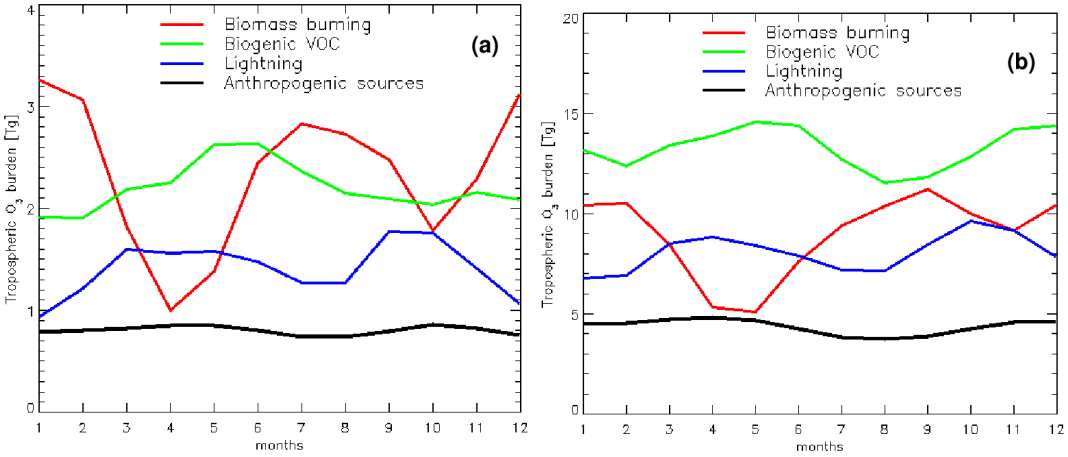

Fig. 7. 5-year monthly mean contribution of the African emissions to **(a)** African and **(b)** global tropospheric ozone burden ($Tg\,O_3$). Note the difference in the scales.

ACPD
6, 5797–5838, 2006

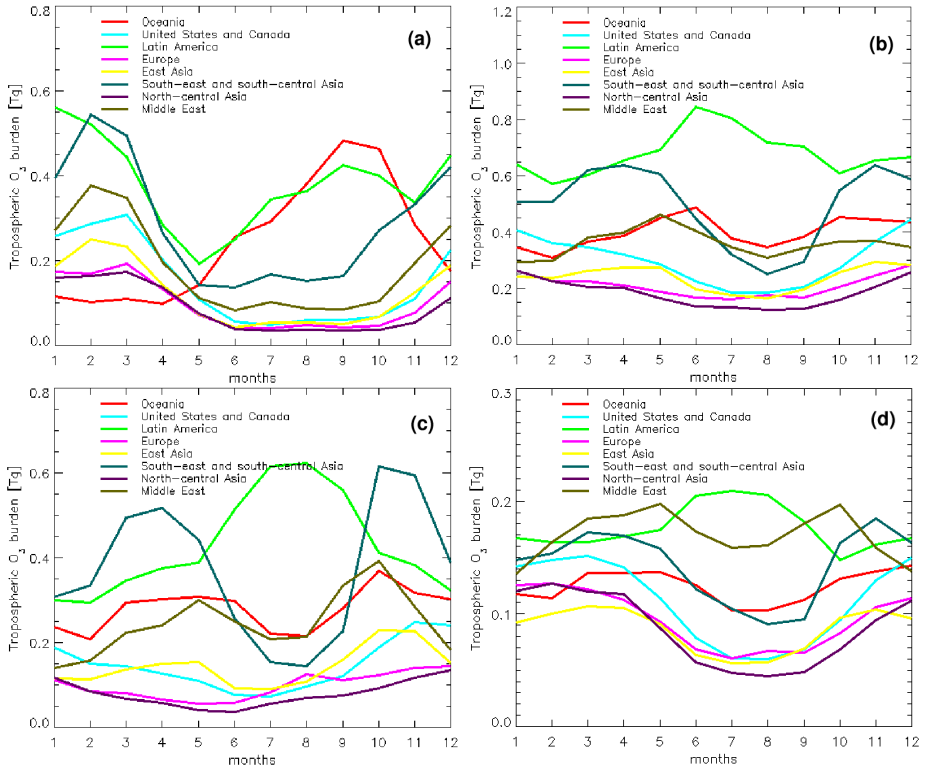

Fig. 8. Seasonal variation of the contribution of African **(a)** biomass burning, **(b)** biogenic VOC, **(c)** lightning and **(d)** anthropogenic emissions to the tropospheric ozone burden ($Tg\,O_3$) of different regions of the world. Note the different scales.

ACPD
6, 5797–5838, 2006

EGU

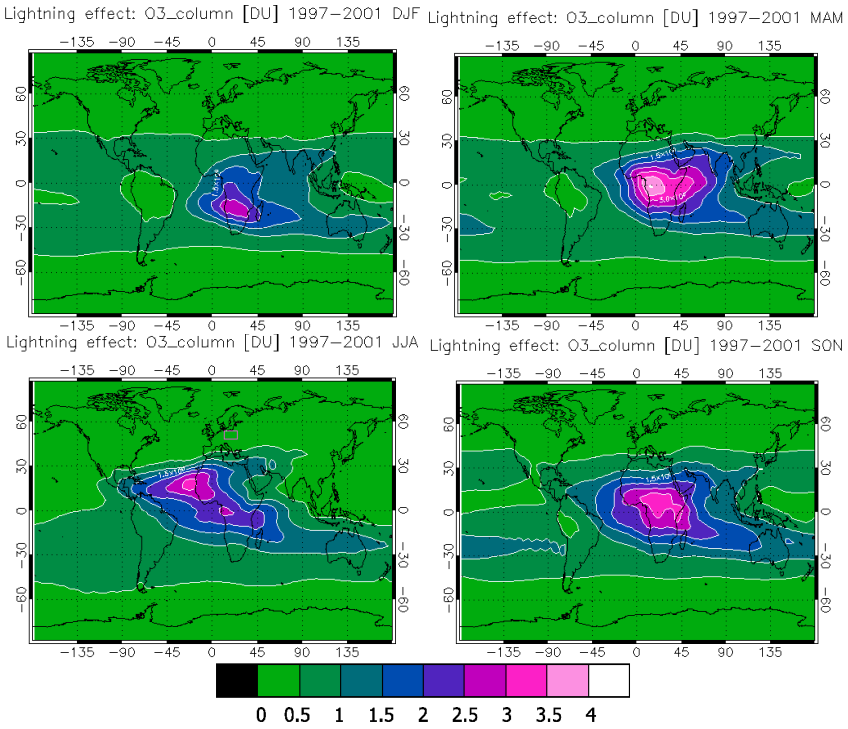

Fig. 9. Tropospheric ozone column (DU) produced by African lightning NO_x emissions. Plots show the difference between the reference simulation and the simulation without African lightning emissions.

ACPD
6, 5797–5838, 2006